

Entanglement entropy of XX spin 1/2 chain with random partitioning at arbitrary temperature

Mohammad Pouranvari

^aDepartment of Solid-State Physics, Faculty of Science, University of Mazandaran, Babolsar, 4741613534, Iran

Abstract

We study the entanglement properties of random XX spin 1/2 chains at an arbitrary temperature T using random partitioning, where sites of a size-varying subsystem are chosen randomly with a uniform probability p , and then an average over subsystem possibilities is taken. We show analytically and numerically, using the approximate method of real space renormalization group, that random partitioning entanglement entropy for the XX spin chain of size L behaves like $EE(T, p) = a(T, p)L$ at an arbitrary temperature T with a uniform probability p , i.e., it obeys volume law. We demonstrate that $a(T, p) = \ln(2)\langle P_s + P_{t\uparrow\downarrow} \rangle p(1 - p)$, where P_s and $P_{t\uparrow\downarrow}$ are the average probabilities of having singlet and triplet $_{\uparrow\downarrow}$ in the entire system, respectively. We also study the temperature dependence of pre-factor $a(T, p)$. We show that EE with random partitioning reveals both short- and long-range correlations in the entire system.

1. Introduction

Physicists use the entanglement properties of a system (among other characterizations) to understand the system, theoretically and experimentally[1, 2, 3, 4, 5, 6]. The notion of entanglement was born with quantum physics[7, 8], and it has no corresponding concept in classical physics. The entanglement properties capture the non-local properties of the system related to the correlations in the entire system. There are some measures to quantify the entanglement properties of the system, among which we can name the entanglement entropy (EE) (see below for definition). However, there are other measurements such as Renyi entropy, concurrence, logarithmic negativity etc.[1, 9, 10]. It is also possible to measure the entanglement properties of the system experimentally[11, 12, 13]. One of the features that people study is the behavior of the EE versus system size. For example, the EE grows with the boundary of the subsystem (what is called area law) or it grows with the volume of the subsystem (volume law). For free fermions, the area law sometimes is violated[14, 15, 16, 17, 18, 19]. To calculate the EE, one *usually* divides the system into two parts. If the system has L sites, the first $L/2$ sites are the subsystem (sites 1 up to $L/2$), and the rest is called the environment. In this cutting, the amount of entanglement between this specific subsystem and its environment is calculated. Studying the EE with this kind of bi-partitioning has been used before to analyze the behavior of different systems at zero temperatures or a non-zero temperature[20, 21, 22, 23, 24, 25, 26, 27]. Rather than simply cutting the system in the middle, there are also other cutting possibilities that affect the information we can obtain. I.e., for a system with a phase transition, the EE obtained with one form of cutting could reveal the phase transition, while we

get no information about the phase transition with some other cuttings. Thus, *the way we cut the system matters*. See, for example, Refs. [28, 29, 30] where people examined different cuttings in bi-partitioning. Thus, to acquire all the entanglement properties of the system, we would divide it in all possible ways. In this regard, we use the notion of *random partitioning*, in which we take an average over the EE's corresponding to the randomly chosen subsystems. More accurately, to obtain random-partitioning EE, we do the following: first, we attribute a probability to each site based on a probability distribution, i.e., sites that belong to the subsystem are chosen randomly. Moreover, subsystem size varies between 1 to L (there are $\binom{n}{L}$ different forms of having subsystems with n sites). We consider all of these ways of partitioning, and we take an average of the EE corresponding to them. This way of partitioning is entirely different from the usual method of bi-partitioning. In the bi-partitioning, the system's middle is the boundary between the subsystem and its environment. In contrast, in the random bi-partitioning, there are many boundaries at different points. As a limiting case, if the subsystem sites are every other spin, we expect a volume law for the entanglement entropy.

Recently, this form of partitioning has been used for the *ground state* of a *clean*, free fermion system[31]. They found a volume law dependence of the EE to the system size with a logarithmic correction term. Also, people studied the entanglement spectrum under random partitioning[32]. Here, we advance these previous studies in two directions. First, we consider a *disordered* system with random impurities and second, we are concerned mainly with a *typical excited state* at an arbitrary temperature T .

By analytical and numerical investigations, we find that the behavior of the EE with a random partitioning is volume law: $EE(T, p) = a(T, p)L$, with a pre-factor a that depends on the probability and temperature. We obtain the analytical form for

Email address: m.pouranvari@umz.ac.ir (Mohammad Pouranvari)

$a(T, p)$ and verify it numerically. We show that the behavior of $a(T, p)$ is related to the number of entangled bonds in the entire system. We finally discuss that EE in the random partitioning reveals the short-range and the long-range correlations in the entire system.

The rest of the paper is separated into two parts; in the first part, section 2, we introduce the XX model and the method to calculate the EE. The calculations are based on the approximate method of real space renormalization group for the ground state (RSRG) and a typical excited state (RSRG-X). We explain these methods in the following section. We then analytically prove the behavior of the EE in random partitioning with a uniform probability. The numerical evaluations and verification of the behavior of the EE are presented in section 3. Based on these calculations, we give a picture of the EE in random partitioning and conclude in section 4.

2. Analytical evaluation

We consider a one-dimensional XX spin 1/2 chain with L spins. They are coupled together locally and with random strength. Hamiltonian of the system is:

$$H = \sum_{n=1}^{L-1} J_n (s_n^x s_{n+1}^x + s_n^y s_{n+1}^y). \quad (1)$$

(with open boundary condition) where J_n are distributed randomly by a distribution function (to be determined later). The entanglement properties of this model have been studied before [33, 34, 35, 36].

We want to obtain the entanglement properties of this model, and to do so, we use the notion of EE. In a *bi-partitioned system*, where the system is divided into two parts: subsystem A and its environment, the EE is the von Neumann entropy of the reduced density matrix of the subsystem:

$$\text{EE} = -\text{Tr}[\rho_A \ln \rho_A], \quad (2)$$

where ρ_A is the reduced density matrix for the subsystem A obtained by tracing out the environment degrees of freedom from the density matrix ρ of the entire system. For a pure state the density matrix is $\rho = |\Psi\rangle\langle\Psi|$, where $|\Psi\rangle$ is the state of the system. Thus, to calculate the EE in a bi-partitioned system in a brute-force method, first, we need to diagonalize the Hamiltonian to obtain its eigenvalues and eigenvectors $\{|\Psi\rangle\}$. Then, by calculating the reduced density matrix of a chosen subsystem and using Eq. (2), we obtain the EE. To obtain the system's state in the XX spin 1/2 chain with L spins, one deals with matrices with size 2^L , which exponentially growing with the system size. By Jordan-Wigner transformation, the XX model is transformed into a free fermion model, where the size of the matrices to deal with in numerical calculations reduces to L [37, 38]. In addition to this direct and exact method, the XX spin 1/2 chain has been studied by approximate methods such as the real space renormalization group (RSRG) method [39, 40, 41]. In this method, the *approximate* ground state of a *random* XX spin 1/2 chain is obtained. An extension of this method is also developed to obtain an approximate typical *excited state*, namely

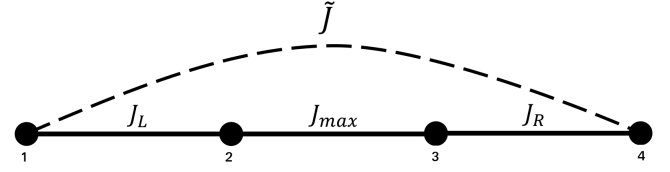


Figure 1: A part of the spin chain is presented in which we assume $J_{\max} > J_L, J_R$. In real space renormalization group method, after picking up J_{\max} , we remove spin 2 and 3 and couple spin number 1 and 4 with $\tilde{J} = \frac{J_L J_R}{J_{\max}}$.

the RSRG-X. We use these approximate methods to calculate the EE in random partitioning.

We should note that, in this paper, we do not use the corresponding free fermion model of Eq. (1) to obtain the EE in random partitioning. Using the free fermion method in calculating EE for disjoint blocks is incorrect (since the Jordan-Wigner transformation of i th site depends on the previous sites). Instead, we use RSRG/RSRG-X approximate method to obtain EE, which is based on the number of singlets and triplets that cross the boundary of the subsystem. These methods do not fail for a disjoint subsystem. In what follows, we explain both methods and describe how to use them to calculate approximately the EE.

2.1. Real space renormalization group

To obtain the approximate ground state of a XX spin 1/2 chain by RSRG method, we go through the following steps [42]. Consider the Hamiltonian of Eq. (1) in which coupling constants $\{J\}$ are distributed randomly. First, we pick up the largest coupling J_{\max} . In the ground state of the system, we put the two spins that are coupled with J_{\max} in a *singlet state* $|\text{singlet}\rangle = \frac{1}{\sqrt{2}}[|\uparrow\downarrow\rangle - |\downarrow\uparrow\rangle]$. Next, we remove these two spins and couple the two closest spins with an effective coupling $\tilde{J} = \frac{J_L J_R}{J_{\max}}$ (see Fig.1 for a schematic representation).

By repeating this process, the selected spin pairs are in the singlet state. Thus, the ground state of the system is the direct product of singlets with arbitrary bond length (the so-called random singlet phase). Since \tilde{J} is smaller than both of J_L, J_R , by repeating the RSRG process, we will get smaller and smaller values for \tilde{J} . So, the probability of $\{J\}$ distributions will be a power-law: $P(J) = \alpha J^{\alpha-1}$ for $0 \leq J \leq 1$. The RSRG fixed point is the infinite randomness fixed point and corresponds to $\alpha \rightarrow 0$. In this regard, small values of α correspond to the strong disorder regime that RSRG yields to an asymptotically correct ground state.

For a highly excited state, a modified version of the RSRG is developed, namely the RSRG-X [43]. We should note that, at $T = 0$, the state of the system is pure and we obtained it approximately using the RSRG method, which in this approximation is the product state of the singlet state pairs. On the other hand, for $T \neq 0$, the state of the system is mixed which represents a combination of possible states weighted with a probability. In this paper, we do not consider a mixed state for a non-zero temperature, but we consider a typical state which is one of the possible states. This typical state (which in the RSRG-X approximation is a product state of singlet and each of the triplet

Table 1: The effective coupling based on the chosen eigen-state of two spins and the corresponding energy.

Eigen-state	Eigenvalue	Probability	Effective coupling
singlet = $\frac{1}{\sqrt{2}}[\uparrow\downarrow\rangle - \downarrow\uparrow\rangle]$	$-J/2$	$\frac{1}{Z}e^{J/2T}$	$\tilde{J} \approx +\frac{J_L J_R}{J_{\max}}$
triplet $_{\uparrow\downarrow}$ = $\frac{1}{\sqrt{2}}[\uparrow\downarrow\rangle + \downarrow\uparrow\rangle]$	$+J/2$	$\frac{1}{Z}e^{-J/2T}$	$\tilde{J} \approx +\frac{J_L J_R}{J_{\max}}$
triplet $_{\uparrow\uparrow}$ = $ \uparrow\uparrow\rangle$	0	$\frac{1}{Z}$	$\tilde{J} \approx -\frac{J_L J_R}{J_{\max}}$
triplet $_{\downarrow\downarrow}$ = $ \downarrow\downarrow\rangle$	0	$\frac{1}{Z}$	$\tilde{J} \approx -\frac{J_L J_R}{J_{\max}}$

states) is a pure one and the notion of the EE can be used to quantify the entanglement properties in the system.

In the RSRG-X method, we look for the two spins that are coupled with the largest magnitude value, and put them in the singlet state or each of the triplet states based on the Boltzmann distribution function:

$$P_B = \frac{1}{Z} \exp(-E/T), \quad (3)$$

where E is the energy of the singlet/triplet state of the two spins, and $Z = 2 + 2 \cosh \frac{J}{2T}$ to have a normalized probability (see Table 1 [22]).

The effective coupling, \tilde{J} depends on which singlet or triplets are chosen by the Boltzmann distribution. In doing the RSRG-X method, the probability of getting smaller magnitude values for couplings increases, and thus we have a power-law distribution:

$$P(J) = \frac{\alpha}{2} |J|^{\alpha-1}, \text{ for } |J| \leq 1 \quad (4)$$

Like the RSRG method, the fixed point corresponds to $\alpha \rightarrow 0$ and the strong disorder regime, where the RSRG-X is asymptotically correct, corresponds to small values of α . The outcome of the RSRG-X method, a typical excited state, is the direct product of singlets and triplets. We work in the sector of half-filling in the corresponding free fermion representation, which is equivalent to $S_z^{\text{total}} = 0$ in the spin representation of the Hamiltonian.

We note that the singlet and triplet $_{\uparrow\downarrow}$ states are entangled states with the value of the EE equal to $\ln(2)$; but triplet $_{\uparrow\uparrow}$ and triplet $_{\downarrow\downarrow}$ states are not entangled. Since the ground state (a typical excited state) of the system in the RSRG (RSRG-X) method is the product state of singlets (singlets and triplets), only those singlets (singlets and triplet $_{\uparrow\downarrow}$) that *cross the boundary* contribute to the EE. Thus, for a bi-partitioned system, to calculate the EE, we count the number of singlets (number of singlets and triplet $_{\uparrow\downarrow}$) crossing the boundary and multiply it by $\ln(2)$ [44, 34]. The numerical verification of the RSRG and RSRG-X methods to calculate the EE have been studied before [45, 46, 36, 22].

At $T = 0$, all spins that are decimated in the RSRG method are in the singlet state. Namely, the probability of having a singlet, P_s is 1, and the probability of having each of the triplets is 0. Thus we expect $L/2$ singlets across the entire system. On the other hand, we expect that each of the singlet and the triplets are chosen with the same probability for a large T in the RSRG-X method. I.e., $P_s = P_{t_{\uparrow\downarrow}} = P_{t_{\uparrow\uparrow}} = P_{t_{\downarrow\downarrow}} = \frac{1}{4}$. See Table 1. As $T \rightarrow \infty$, the Boltzmann probability of the singlet and triplets are

the same. Therefore, there are $L/4$ singlets and $L/4$ triplet $_{\uparrow\downarrow}$ s. In addition, for an arbitrary $T \neq 0$, we need to calculate the average probabilities weighted with $P(J)$:

$$\langle P_s \rangle = \int_{-1}^1 dJ P(J) \frac{e^{J/2T}}{Z}, \quad (5)$$

$$\langle P_{t_{\uparrow\downarrow}} \rangle = \int_{-1}^1 dJ P(J) \frac{e^{-J/2T}}{Z}, \quad (6)$$

and thus, the average probability of having a singlet and a triplet $_{\uparrow\downarrow}$ at an arbitrary temperature T is:

$$\langle P_s + P_{t_{\uparrow\downarrow}} \rangle = \alpha(2T)^\alpha \int_0^{\frac{1}{2T}} dx \frac{x^{\alpha-1}}{1 + \text{sech}(x)}. \quad (7)$$

There is no simple analytical solution for this integral, so we will calculate it numerically. Finally, we should note that the RSRG is not an exact method, and it is asymptotically correct [45].

2.2. EE in random partitioning

Now, we explain how to calculate the EE for a bi-partitioned system in which the sites that belong to the subsystem are chosen *randomly*. First, we specify a probability p_i for each site i to belong to the subsystem based on a probability distribution. The subsystem size n , can vary from 1 to L , and for each of them, there are $\binom{L}{n}$ different ways of choosing n sites out of L sites. In addition, for each of these choices, there is a corresponding probability that each of the n sites belongs to the subsystem and other sites do not belong to the subsystem: $\prod_{i \in A} p_i \prod_{i \notin A} (1 - p_i)$. Thus the EE for a specific probability distribution in the random partitioning $EE(T, \{p\})$ is the following [31]:

$$EE(T, \{p\}) = \sum_{n=1}^{L-1} \sum_{j=1}^{\binom{L}{n}} EE_n^j(T) \left(\prod_{i \in A} p_i \right) \left(\prod_{i \notin A} (1 - p_i) \right), \quad (8)$$

where EE_n^j is one of the $\binom{L}{n}$ calculated EE's corresponding to the case of having n sites in the subsystem.

In the particular case of uniform probability, where the probability for each site to belong to the subsystem is the same for all sites ($p_i = \text{constant} = p$) we can use the above equation to obtain the EE in random partitioning with constant probability distribution $EE(T, p)$:

$$EE(T, p) = \sum_{n=1}^{L-1} \sum_{j=1}^{\binom{L}{n}} EE_n^j(T) p^n (1 - p)^{L-n}. \quad (9)$$

In practice, we can not go over all samples of $\binom{L}{n}$ choices for a large L ; instead, we take the average over enough large number of samples to obtain \overline{EE}_n , and thus we have:

$$EE(T, p) = \sum_{n=1}^{L-1} \overline{EE}_n(T) \binom{L}{n} p^n (1 - p)^{L-n}, \quad (10)$$

Since $\binom{L}{n} = \binom{L}{L-n}$, we can deduce from Eq. (10) that $EE(T, p) = EE(T, 1-p)$, and thus we would expect a symmetric plot for $EE(p)$ versus p about $p = 1/2$.

To obtain an analytical expression for $\overline{EE}_n(T)$, we do the following: at $T = 0$, since the state of the system is pure, we expect that $\overline{EE}_n = \overline{EE}_{L-n}$; thus, we guess that we can write $\overline{EE}_n \propto n(L-n)$. To obtain the proportionality at zero temperature, we note that all bonds are singlet; therefore, having one site as the subsystem will yield to $\overline{EE}_{n=1} = \ln(2) \times 1$; thus the proportionality is $\frac{\ln(2)}{L-1}$, and:

$$\overline{EE}_n(T=0) = \frac{\ln(2)}{L-1} n(L-n). \quad (11)$$

Replacing this result in Eq. (10), we obtain the following expression for the $EE(p)$ at $T = 0$:

$$EE(T=0, p) = \ln(2)p(1-p)L. \quad (12)$$

In addition, for an arbitrary T , as we argued above, on average, only $\langle P_s + P_{t_1} \rangle$ fraction of the bonds contribute to the EE and thus:

$$EE(T, p) = \ln(2)\langle P_s + P_{t_1} \rangle p(1-p)L \quad (13)$$

$$= a(T, p) L \quad (14)$$

where, $a(T, p) = \ln(2)\langle P_s + P_{t_1} \rangle p(1-p)$. In conclusion, we see a volume law expression for the random partitioning EE with $a(T, p)$ as the pre-factor as a function of temperature and probability. We present numerical calculations in the next section that verify our analytical results.

3. Numerical verification

In our numerical calculations of the EE in a random partitioning with a uniform probability, we do the following. First, we apply the RSRG/RSRG-X to obtain the approximate ground state/typical excited state of the system corresponding to a specific system size. To work in the strong disorder regime where the RSRG method is asymptotically correct, we set $\alpha = 0.2$. Then we randomly choose sites that belong to the subsystem. By counting the number of singlets and triplet_{↑↓}s that cross the boundary of the chosen subsystem, we calculate EE for that chosen subsystem. We repeat this process large enough times and calculate its average \overline{EE}_n . In the RSRG-X process, since each singlet or triplet is chosen based on the Boltzmann distribution, we need to take the ensemble average for each temperature T . In addition, since the coupling constants are random, we also take the disorder average over random $\{J\}$ realizations. After doing these averaging calculations, the $EE(T, p)$ is obtained.

First, we check the symmetric property of $\overline{EE}_n = \overline{EE}_{L-n}$, meaning that the \overline{EE}_n has to be symmetric about $n = L/2$. In addition, we compare the \overline{EE} calculated numerically with Eq. (11). As we can see in Fig. 2, the plot of \overline{EE} numerically obtained is symmetric about $L/2$, and also it fairly matches with Eq. (11).

Next, we check the L dependence of the $EE(T, p)$. We plot the numerical data of EE versus system size L and the fitted straight line. This comparison is plotted in Fig. 3 for different temperatures and probabilities. The sum of squared residuals of the least squares fits are also denoted; since they have very small values, we can conclude that the straight-fitted lines are fitted the numerical data very well. As a double check, we also fit the logarithm of the EE versus the logarithm of the system size with a straight line, and we find that the slope is very close to 1 (see Fig. 4). Thus, we conclude that $EE \propto L$, i.e., the EE has power-law behavior for system size L .

Now that we know the system size dependence is a power-law with power 1, we write $EE = a(T, p)L + c$ (we add the y-intercept c to be determined with numerical calculations) and study the behavior of coefficient a and c as a function of temperature T and probability p . One way to do this, is to fit the data of EE versus L with a straight line and obtain the slope and the y-intercept of the fitted line numerically. The results of these calculations are plotted in Figs. 5 and 6. From the behavior of a versus probability, we can see that it is symmetric about $p = 1/2$, consistent with the analytical result of Eq. (13) (see left panel of Fig. 5).

In addition, from the behavior of a versus temperature, we can see that it approaches constant values at low and high temperatures. These constants are consistent with the analytical values of a in Eq. (14), which are $\ln(2) \times p(1-p)$ in low temperatures, and $\frac{1}{2} \ln(2) \times p(1-p)$ for high temperatures (Since $\langle P_s + P_{t_1} \rangle$ goes to 1 in the low T limit and it goes to $\frac{1}{2}$ in the high T limit. See the middle panel of Fig. 5).

In the right panel of Fig. 5, we do the following. First, for the numerically obtained values of a , we plot $\frac{a}{p(1-p)}$ for some selected values of p . As we can see, they all coincide with each other. I.e., the only probability dependence is in the form of $p(1-p)$. In addition, we can see that the numerically obtained value of a goes to $\ln(2)$ in the low T limit, and it goes to $\frac{1}{2} \ln(2)$ in the high T limit, which are consistent with the analytical result of the $\frac{a}{p(1-p)} = \ln(2)\langle P_s + P_{t_1} \rangle$. For an arbitrary temperature T , numerical data and the analytical predictions of a are in a fair agreement. The difference between the numerically and analytically obtained values of a stems from the fact that we use an approximate RSRG method to calculate the EE. We also note that, in a numerical calculation, it is always possible to benefit from larger system sizes to avoid finite-size scaling. Finally, we can see that the numerically obtained values of c plotted in Fig. 6, are very small compared to the EE values; they are thus negligible.

4. conclusion and outlook

The usual way of measuring the entanglement properties of a system is to bipartite it into two subsystems, and then obtain the *non-local* entanglement properties by calculating the EE. What we did in this paper is distinct: each site has a chance to be part of the subsystem, subsystem size is also varying, and in addition, for each subsystem size, we do all different ways of partitioning, and then we take the average over the calculated EE's.

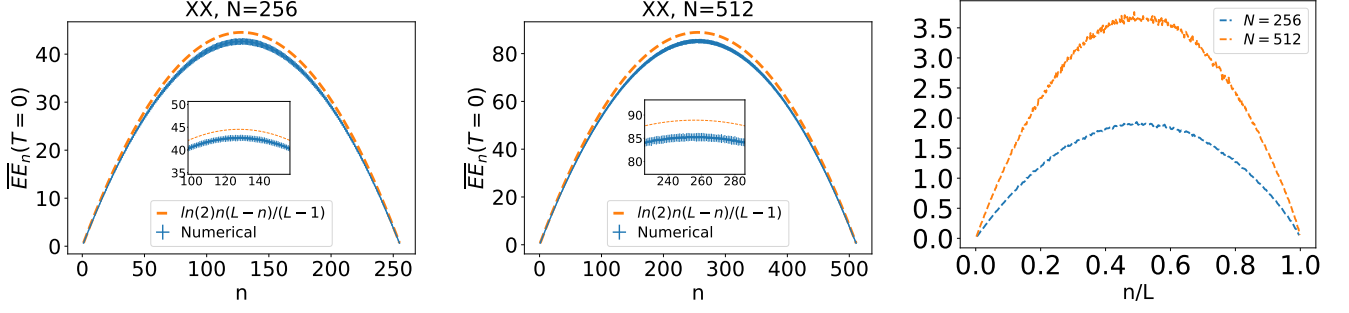


Figure 2: Plot of \overline{EE}_n versus system size n at $T = 0$. In the left panel, we set $N = 256$ and in the middle panel, we set $N = 512$. Plots are symmetric about $n = L/2$ (standard deviations are included). In the right panel, we plot the difference between the numerical and analytical results of Eq. (11) versus n/L . The numerical results fairly matches the analytical results for subsystem sizes n close to 1 and L and it deviates from analytical results about $n \sim L/2$ (See the inset plots. The deviation is less than 4%). For each data point, we take disorder average over $\sim 10^2$ samples, subsystem average over $\sim 10^2$ samples, and thus we take the average over $\sim 10^4$ samples in total.

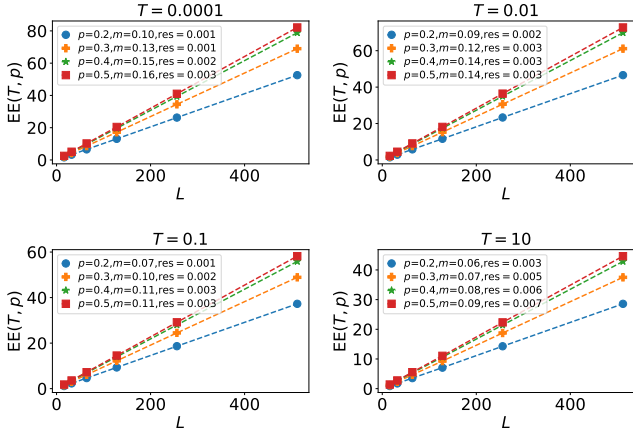


Figure 3: Plot of $EE(T, p)$ versus system size L at fixed temperatures T for some selected values of uniform probabilities p . For each probability p , the slope of the fitted straight line with the obtained numerical results of EE is denoted as m . Also, the sum of squared residuals of the least squares fits is denoted as 'res'. Small values for res, denote the fact that the straight lines are a good fit for the numerical data. For each data point, we take disorder average over $\sim 10^2$ samples, subsystem average over $\sim 10^2$ samples, ensemble average over ~ 10 samples, and thus we take the average over $\sim 10^5$ samples in total.

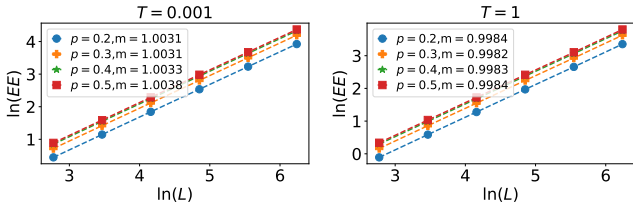


Figure 4: Plot of the $\ln(EE)$ versus $\ln(L)$ at two fixed temperature T for some values of probability p . The slope of the straight fitted line is denoted as m . For each data point, we take disorder average over $\sim 10^2$ samples, subsystem average over $\sim 10^2$ samples, ensemble average over ~ 10 samples and thus we take the average over $\sim 10^5$ samples in total.

In such wise, we measure long-range as well as short-range correlations in the system. In other words, when we calculate the EE for a bi-partitioned system, we measure how much subsystem is entangled with the environment, in which long-range correlations and also near-to-the-boundary short-range correlations take part. On the other hand, we are measuring both the short-range and long-range correlations in the entire system when we randomly partition the system in all possible ways,

Considering the XX spin chain, if we cut the system in the middle and then calculate the EE , we are counting the number of entangled bonds (singlet and triplet $_{\uparrow\downarrow}$) that cross the middle of the system, and thus we are counting the long bonds or those short bonds that are close to the boundary. But, since in random partitioning the partitions are random and they can be disconnected as well, we are counting the entangled bonds, both with short and long lengths. In averaging over all such partitioning, we thus count the number of singlets and triplet $_{\uparrow\downarrow}$ *all over the entire system*. This is, of course, in agreement with the analytical point of view that $N_s + N_{t_{\uparrow\downarrow}} = \langle P_s + P_{t_{\uparrow\downarrow}} \rangle \times \frac{L}{2}$, and thus we can rewrite the $EE(T, p)$ of Eq. (13) as the following:

$$EE(T, p) = 2 \ln(2)p(1-p)(N_s + N_{t_{\uparrow\downarrow}}) \quad (15)$$

In Fig. 7, we plot the number of singlets and triplet $_{\uparrow\downarrow}$ s forming in the entire system as a function of the temperature. In the low T limit, all bonds are only singlet and triplet $_{\uparrow\downarrow}$, and the sum goes to $L/2$. On the other hand, in the high-temperature limit, the singlet and the three triplets have the same probability, so the sum goes to $L/8$. As a numerical check, we also plot and compare Eq. (15) with the numerically obtained data for the EE . We see full agreement.

The XX spin chain, which we employed in this paper, gives us a schematic representation of the bonds forming in the system. However, this picture is not always available. So in general, to see both short- and long- range-correlations, we can use the random partitioning method. In particular, the behavior of the EE in a Hamiltonian with local and non-local interactions would be interesting. The random partitioning can also be used in characterizations of the phase transition. For example, in the Anderson delocalized-localized phase transition[47].

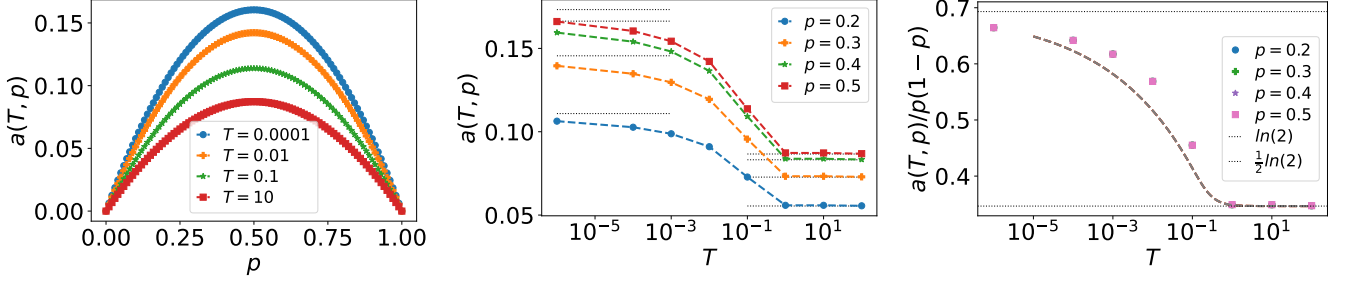


Figure 5: The EE versus system size L is fitted with the straight line $aL + c$, and the results of the behavior of a as a function of probability (left panel) and temperature (middle panel) are plotted. In the middle panel, the horizontal lines are $\ln(2)p(1-p)$ and $\frac{1}{2}\ln(2)p(1-p)$ for each p . In the right panel, the numerically obtained $\frac{a}{p(1-p)}$ are plotted for different probabilities, p . We can see that they coincide. In addition, The result of the analytically obtained $\frac{a}{p(1-p)}$ based on Eq. (13), is plotted with a dashed line. These two numerical and analytical results nearly match. Two horizontal lines of $\ln(2)$ and $\frac{1}{2}\ln(2)$ are also plotted. For each data point, we take disorder average over $\sim 10^2$ samples, subsystem average over $\sim 10^2$ samples, ensemble average over ~ 10 samples and thus we take the average over $\sim 10^5$ samples in total.

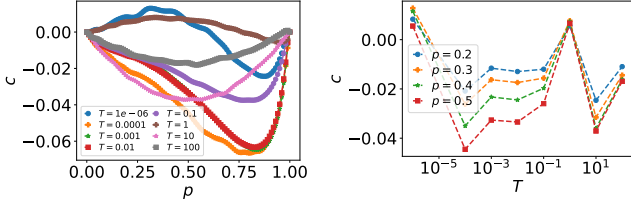


Figure 6: The EE versus system size L is fitted with the straight line $aL + c$, and the results of the y-intercept behavior c as a function of the probability (left panel) and also temperature (middle panel) are plotted. The values of the numerically obtained c are smaller than 10^{-2} which is much smaller than the value for the EE. For each data point, we take disorder average over $\sim 10^2$ samples, subsystem average over $\sim 10^2$ samples, ensemble average over ~ 10 samples and thus we take the average over $\sim 10^5$ samples in total.

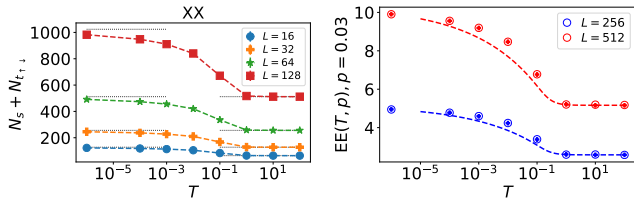


Figure 7: Left panel: Number of singlets and triplet₁s forming all over the entire system versus temperature T . Horizontal lines are $L/2$ and $L/8$. Right panel: three different data are plotted: the numerically obtained data of the EE denoted by an unfilled circles, $\ln(2)\langle P_s + P_{t1} \rangle p(1-p)L$ with a dashed line, and $2\ln(2)p(1-p)(N_s + N_{t1})$ with a plus sign. For each data point, we take disorder average over $\sim 10^2$ samples, subsystem average over $\sim 10^2$ samples, ensemble average over ~ 10 samples and thus we take the average over $\sim 10^5$ samples in total.

Besides, we only considered the uniform probability distribution, i.e., each site has the same chance to belong to the subsystem. Considering non-uniform probabilities could also be helpful and give us more physical insights.

acknowledgments

The author thanks Dr. Jahanfar Abouei for valuable discussions. The author gratefully acknowledges the high performance computing center of the university of Mazandaran for providing computing resources and time. This work is based upon research funded by Iran National Science Foundation (INSF) under project No. 4000258.

References

- [1] R. Horodecki, P. Horodecki, M. Horodecki, K. Horodecki, Quantum entanglement, Rev. Mod. Phys. 81 (2009) 865–942. doi:10.1103/RevModPhys.81.865. URL <https://link.aps.org/doi/10.1103/RevModPhys.81.865>
- [2] N. Laflorencie, Quantum entanglement in condensed matter systems, Physics Reports 646 (2016) 1 – 59. doi:https://doi.org/10.1016/j.physrep.2016.06.008. URL <http://www.sciencedirect.com/science/article/pii/S0370157316301582>
- [3] L. H. Kauffman, S. J. Lomonaco, Quantum entanglement and topological entanglement, New Journal of Physics 4 (2002) 73–73. doi:10.1088/1367-2630/4/1/373. URL <https://doi.org/10.1088/1367-2630/4/1/373>
- [4] D.-L. Deng, X. Li, S. Das Sarma, Quantum entanglement in neural network states, Phys. Rev. X 7 (2017) 021021. doi:10.1103/PhysRevX.7.021021. URL <https://link.aps.org/doi/10.1103/PhysRevX.7.021021>
- [5] A. Kitaev, J. Preskill, Topological entanglement entropy, Phys. Rev. Lett. 96 (2006) 110404. doi:10.1103/PhysRevLett.96.110404. URL <https://link.aps.org/doi/10.1103/PhysRevLett.96.110404>
- [6] P. Calabrese, J. Cardy, Entanglement entropy and quantum field theory, Journal of Statistical Mechanics: Theory and Experiment 2004 (06) (2004) P06002. doi:10.1088/1742-5468/2004/06/p06002. URL <https://doi.org/10.1088/1742-5468/2004/06/p06002>
- [7] A. Einstein, B. Podolsky, N. Rosen, Can quantum-mechanical description of physical reality be considered complete?, Phys. Rev. 47 (1935) 777–780. doi:10.1103/PhysRev.47.777. URL <https://link.aps.org/doi/10.1103/PhysRev.47.777>

- [8] E. Schrödinger, Discussion of probability relations between separated systems, *Mathematical Proceedings of the Cambridge Philosophical Society* 31 (4) (1935) 555–563. doi:10.1017/S0305004100013554.
- [9] S. Szalay, Multipartite entanglement measures, *Phys. Rev. A* 92 (2015) 042329. doi:10.1103/PhysRevA.92.042329.
URL <https://link.aps.org/doi/10.1103/PhysRevA.92.042329>
- [10] V. Vedral, M. B. Plenio, M. A. Rippin, P. L. Knight, Quantifying entanglement, *Phys. Rev. Lett.* 78 (1997) 2275–2279. doi:10.1103/PhysRevLett.78.2275.
URL <https://link.aps.org/doi/10.1103/PhysRevLett.78.2275>
- [11] J. M. Raimond, M. Brune, S. Haroche, Manipulating quantum entanglement with atoms and photons in a cavity, *Rev. Mod. Phys.* 73 (2001) 565–582. doi:10.1103/RevModPhys.73.565.
URL <https://link.aps.org/doi/10.1103/RevModPhys.73.565>
- [12] E. Cornfeld, E. Sela, M. Goldstein, Measuring fermionic entanglement: Entropy, negativity, and spin structure, *Phys. Rev. A* 99 (2019) 062309. doi:10.1103/PhysRevA.99.062309.
URL <https://link.aps.org/doi/10.1103/PhysRevA.99.062309>
- [13] C. A. Sackett, D. Kielpinski, B. E. King, C. Langer, V. Meyer, C. J. Myatt, M. Rowe, Q. A. Turchette, W. M. Itano, D. J. Wineland, C. Monroe, Experimental entanglement of four particles, *Nature* 404 (2000) 256 EP –.
URL <http://dx.doi.org/10.1038/35005011>
- [14] J. Eisert, M. Cramer, M. B. Plenio, Colloquium: Area laws for the entanglement entropy, *Rev. Mod. Phys.* 82 (2010) 277–306. doi:10.1103/RevModPhys.82.277.
URL <https://link.aps.org/doi/10.1103/RevModPhys.82.277>
- [15] M. M. Wolf, Violation of the entropic area law for fermions, *Phys. Rev. Lett.* 96 (2006) 010404. doi:10.1103/PhysRevLett.96.010404.
URL <https://link.aps.org/doi/10.1103/PhysRevLett.96.010404>
- [16] G. Vitagliano, A. Riera, J. I. Latorre, Volume-law scaling for the entanglement entropy in spin-1/2 chains, *New Journal of Physics* 12 (11) (2010) 113049. doi:10.1088/1367-2630/12/11/113049.
URL <https://doi.org/10.1088/1367-2630/12/11/113049>
- [17] M. Pouranvari, K. Yang, Maximally entangled mode, metal-insulator transition, and violation of entanglement area law in noninteracting fermion ground states, *Phys. Rev. B* 89 (2014) 115104. doi:10.1103/PhysRevB.89.115104.
URL <https://link.aps.org/doi/10.1103/PhysRevB.89.115104>
- [18] T. Koffel, M. Lewenstein, L. Tagliacozzo, Entanglement entropy for the long-range ising chain in a transverse field, *Phys. Rev. Lett.* 109 (2012) 267203. doi:10.1103/PhysRevLett.109.267203.
URL <https://link.aps.org/doi/10.1103/PhysRevLett.109.267203>
- [19] B. Swingle, Entanglement entropy and the fermi surface, *Phys. Rev. Lett.* 105 (2010) 050502. doi:10.1103/PhysRevLett.105.050502.
URL <https://link.aps.org/doi/10.1103/PhysRevLett.105.050502>
- [20] G. Wong, I. Klich, L. A. P. Zayas, D. Vaman, Entanglement temperature and entanglement entropy of excited states, *Journal of High Energy Physics* 2013 (12) (2013) 20. doi:10.1007/JHEP12(2013)020.
URL [https://doi.org/10.1007/JHEP12\(2013\)020](https://doi.org/10.1007/JHEP12(2013)020)
- [21] V. Alba, M. Fagotti, P. Calabrese, Entanglement entropy of excited states, *Journal of Statistical Mechanics: Theory and Experiment* 2009 (10) (2009) P10020. doi:10.1088/1742-5468/2009/10/p10020.
URL <https://doi.org/10.1088/1742-5468/2009/10/p10020>
- [22] Y. Huang, J. E. Moore, Excited-state entanglement and thermal mutual information in random spin chains, *Phys. Rev. B* 90 (2014) 220202. doi:10.1103/PhysRevB.90.220202.
URL <https://link.aps.org/doi/10.1103/PhysRevB.90.220202>
- [23] J. Bhattacharya, M. Nozaki, T. Takayanagi, T. Ugajin, Thermodynamical property of entanglement entropy for excited states, *Phys. Rev. Lett.* 110 (2013) 091602. doi:10.1103/PhysRevLett.110.091602.
URL <https://link.aps.org/doi/10.1103/PhysRevLett.110.091602>
- [24] A. Jafarizadeh, M. A. Rajabpour, Bipartite entanglement entropy of the excited states of free fermions and harmonic oscillators, *Phys. Rev. B* 100 (2019) 165135. doi:10.1103/PhysRevB.100.165135.
URL <https://link.aps.org/doi/10.1103/PhysRevB.100.165135>
- [25] J. Rodríguez-Laguna, J. Dubail, G. Ramírez, P. Calabrese, G. Sierra, More on the rainbow chain: entanglement, space-time geometry and thermal states, *Journal of Physics A: Mathematical and Theoretical* 50 (16) (2017) 164001. doi:10.1088/1751-8121/aa6268.
URL <https://dx.doi.org/10.1088/1751-8121/aa6268>
- [26] N. Samos Sáenz de Buruaga, S. N. Santalla, J. Rodríguez-Laguna, G. Sierra, Piercing the rainbow state: Entanglement on an inhomogeneous spin chain with a defect, *Phys. Rev. B* 101 (2020) 205121. doi:10.1103/PhysRevB.101.205121.
URL <https://link.aps.org/doi/10.1103/PhysRevB.101.205121>
- [27] G. Ramírez, J. Rodríguez-Laguna, G. Sierra, Entanglement in low-energy states of the random-hopping model, *Journal of Statistical Mechanics: Theory and Experiment* 2014 (7) (2014) P07003. doi:10.1088/1742-5468/2014/07/P07003.
URL <https://dx.doi.org/10.1088/1742-5468/2014/07/P07003>
- [28] N. Ahmadi, J. Abouie, R. Haghshenas, Frustrated mixed-spin ladders: An intermediate phase between rung-singlet and haldane phases (2021). arXiv:2106.07940.
- [29] Z. Moradi, J. Abouie, Entanglement spectrum of fermionic bilayer honeycomb lattice: Hofstadter butterfly, *Journal of Statistical Mechanics: Theory and Experiment* 2016 (11) (2016) 113101. doi:10.1088/1742-5468/2016/11/113101.
URL <https://doi.org/10.1088/1742-5468/2016/11/113101>
- [30] N. Ahmadi, J. Abouie, D. Baeriswyl, Topological and nontopological features of generalized su-schrieffer-heeger models, *Phys. Rev. B* 101 (2020) 195117. doi:10.1103/PhysRevB.101.195117.
URL <https://link.aps.org/doi/10.1103/PhysRevB.101.195117>
- [31] G. Rośsz, I. A. Kovács, F. Iglói, Entanglement entropy of random partitioning, *The European Physical Journal B* 93 (1) (2020) 8. doi:10.1140/epjb/e2019-100496-y.
URL <https://doi.org/10.1140/epjb/e2019-100496-y>
- [32] S. Vijay, L. Fu, Entanglement spectrum of a random partition: Connection with the localization transition, *Phys. Rev. B* 91 (2015) 220101. doi:10.1103/PhysRevB.91.220101.
URL <https://link.aps.org/doi/10.1103/PhysRevB.91.220101>
- [33] M. Fagotti, P. Calabrese, J. E. Moore, Entanglement spectrum of random-singlet quantum critical points, *Phys. Rev. B* 83 (2011) 045110. doi:10.1103/PhysRevB.83.045110.
URL <https://link.aps.org/doi/10.1103/PhysRevB.83.045110>
- [34] G. Refael, J. E. Moore, Criticality and entanglement in random quantum systems, *Journal of Physics A: Mathematical and Theoretical* 42 (50) (2009) 504010. doi:10.1088/1751-8113/42/50/504010.
URL <https://doi.org/10.1088/1751-8113/42/50/504010>
- [35] Y. Mohdeb, J. Vahedi, S. Kettemann, Excited-eigenstate entanglement properties of xx spin chains with random long-range interactions (2022). arXiv:2201.10607.
- [36] N. Laflorencie, Scaling of entanglement entropy in the random singlet phase, *Phys. Rev. B* 72 (2005) 140408. doi:10.1103/PhysRevB.72.140408.
URL <https://link.aps.org/doi/10.1103/PhysRevB.72.140408>
- [37] I. Peschel, Calculation of reduced density matrices from correlation functions, *Journal of Physics A: Mathematical and General* 36 (14) (2003) L205.
URL <http://stacks.iop.org/0305-4470/36/i=14/a=101>
- [38] S.-A. Cheong, C. L. Henley, Many-body density matrices for free fermions, *Phys. Rev. B* 69 (2004) 075111. doi:10.1103/PhysRevB.69.075111.

- URL <https://link.aps.org/doi/10.1103/PhysRevB.69.075111>
- [39] C. Dasgupta, S.-k. Ma, Low-temperature properties of the random heisenberg antiferromagnetic chain, *Phys. Rev. B* 22 (1980) 1305–1319. doi:10.1103/PhysRevB.22.1305.
URL <https://link.aps.org/doi/10.1103/PhysRevB.22.1305>
- [40] X. Turkeshi, P. Ruggiero, V. Alba, P. Calabrese, Entanglement equipartition in critical random spin chains, *Phys. Rev. B* 102 (2020) 014455. doi:10.1103/PhysRevB.102.014455.
URL <https://link.aps.org/doi/10.1103/PhysRevB.102.014455>
- [41] F. Iglói, C. Monthus, Strong disorder rg approach – a short review of recent developments, *The European Physical Journal B* 91 (11) (2018) 290. doi:10.1140/epjb/e2018-90434-8.
URL <https://doi.org/10.1140/epjb/e2018-90434-8>
- [42] D. S. Fisher, Random antiferromagnetic quantum spin chains, *Phys. Rev. B* 50 (1994) 3799–3821. doi:10.1103/PhysRevB.50.3799.
URL <https://link.aps.org/doi/10.1103/PhysRevB.50.3799>
- [43] D. Pekker, G. Refael, E. Altman, E. Demler, V. Oganesyan, Hilbert-glass transition: New universality of temperature-tuned many-body dynamical quantum criticality, *Phys. Rev. X* 4 (2014) 011052. doi:10.1103/PhysRevX.4.011052.
URL <https://link.aps.org/doi/10.1103/PhysRevX.4.011052>
- [44] G. Refael, J. E. Moore, Entanglement entropy of random quantum critical points in one dimension, *Phys. Rev. Lett.* 93 (2004) 260602. doi:10.1103/PhysRevLett.93.260602.
URL <https://link.aps.org/doi/10.1103/PhysRevLett.93.260602>
- [45] M. Pouranvari, K. Yang, Entanglement spectrum and entangled modes of random xx spin chains, *Phys. Rev. B* 88 (2013) 075123. doi:10.1103/PhysRevB.88.075123.
URL <https://link.aps.org/doi/10.1103/PhysRevB.88.075123>
- [46] M. Pouranvari, K. Yang, Entanglement spectrum and entangled modes of highly excited states in random xx spin chains, *Phys. Rev. B* 92 (2015) 245134. doi:10.1103/PhysRevB.92.245134.
URL <https://link.aps.org/doi/10.1103/PhysRevB.92.245134>
- [47] M. Pouranvari, Entanglement properties of disordered free fermion systems with random bi-partitioning (2022). doi:10.48550/ARXIV.2208.11409.
URL <https://arxiv.org/abs/2208.11409>